

Convection-Diffusion as a Model of the Early Current in the Giant Axon

JARL V. HÄGGLUND

Institute of Physiology and Medical Biophysics, The Biomedical Centre, Uppsala, Sweden

ABSTRACT

Convection and diffusion in a membrane with a low density of fixed positive charges have been theoretically analysed as a model of the early current in the giant axon. The model can be regarded as a part of Teorell's excitability analogue. The non-linear transient behaviour of the model conductance has been numerically compared with the conductance associated with sodium activation, using Hodgkin & Huxley's equations. The two models show considerable similarities. The sigmoidal increase of the conductance under depolarization and the exponential decay under repolarization is well reproduced by the convection-diffusion model. The time constant of the model conductance is approximately a function of the instantaneous potential, as in the Hodgkin-Huxley theory. The voltage dependence of the time constant is also in agreement with Hodgkin & Huxley. A quantitative comparison has been made, giving the approximate values of the model parameters necessary for compatibility with squid-axon data.

INTRODUCTION

The Hodgkin-Huxley theory (1), describing the electrical behaviour of the giant axon, has been very successful. The mathematical formulation of the theory is an empirical summary of experiments obtained by the voltage-clamp technique. The theoretical equations are capable not only of reproducing the voltage-clamp experiments but also of describing many other properties of the nerve axon. However, the mathematical formulation, as Hodgkin & Huxley also pointed out, is not unique. The detailed explanation of the behaviour of the ionic conductance changes is still an open question. Since the Hodgkin-Huxley theoretical formulation has such a wide generality in predicting experiments, the Hodgkin-Huxley formalism must be considered as an appropriate goal for model systems of the axon membrane (2).

Among the many models discussed in connection with axon behaviour, models based on the Nernst-Planck equations have aroused much interest. Cole (3) has reviewed the electrodiffusion models for passive ion movement through a membrane. He concluded that electrodiffusion processes were unable

to account for many experimental results. Recent investigators (4, 5), however, have shown that electrodiffusion systems have properties which suggest that electrodiffusion may be an important transport mechanism in excitable membranes.

One of the more complete analogues, partly based on the Nernst-Planck equations, is Teorell's membrane oscillator or electrohydraulic excitability analogue (6, 7, 8, 9, 10, 11, 12), which is capable of describing qualitatively many features of excitable tissue.

In Teorell's oscillator an interaction between osmotic, electrical and hydrodynamical forces causes instability phenomena, which have been deduced theoretically and demonstrated experimentally in artificial membranes. The energy to sustain the oscillations is supplied from an externally applied constant current. The relaxation phenomena in the oscillator play an essential role in the origin of the oscillations. The bulk flow or the convection of the fluid across the membrane causes a relaxation in the concentration profile (13), as well as in the pressure. One example of special interest, showing the similarity between Teorell's model and biological observations, is Teorell's application of the voltage-clamp technique to the model (8). The results were obtained from analogue computations, using the theoretical formulation of the model and are in many respects in agreement with Hodgkin & Huxley's experiments. The so-called "early current" and "late outward current" in the formalism of Hodgkin & Huxley can be considered as corresponding respectively to the concentration profile relaxation and the pressure relaxation in Teorell's excitability analogue. Since the first of these two processes in both models is fast, as compared with the latter, it is possible to compare the sodium activation or the early current in the Hodgkin-Huxley model with the relaxation of the concentration profile.

The purpose of the present investigation is to analyse theoretically and numerically the convection and diffusion in a porous membrane with a low, positive, fixed-charge density in the pores as a

model of the conductance changes associated with the sodium activation or the early current under a voltage clamp. This convection-diffusion model is identical with that part of Teorell's membrane oscillator which gives rise to the concentration profile relaxation, which in the following pages will be referred to as "the convection-diffusion relaxation".

In the present analysis a more complete formulation of the convection-diffusion system is used (13), in contrast to the linear first-order approximation of the time-variant resistance used by Teorell. The extended theory is needed to show the detailed nonlinearities discussed in the present paper (cf. p. 246 in ref. 8). However, this extended theory is based on macroscopic laws, which may not be applicable in the narrow pores of the nerve-axon membrane, with a thickness of approximately 100 Å, as discussed by Solomon (14) and recently by Forster (15).

THEORY

The convection-diffusion model

The model considered is shown in Fig. 1a. A membrane containing pores or channels lined with posi-

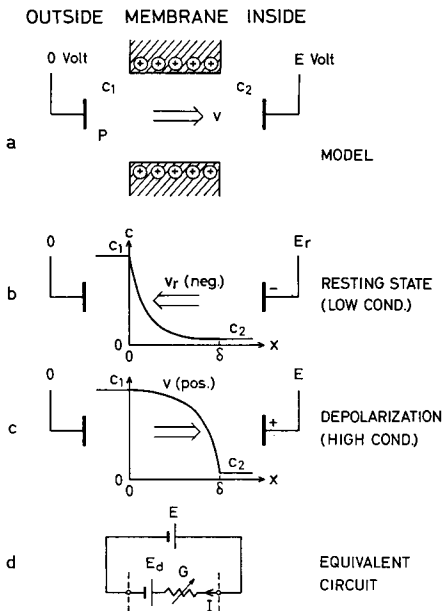


Fig. 1. Model of the axon membrane. (a) Convection-diffusion regime within a pore with fixed positive charges. The external potential difference E creates a convectional flow with velocity V by electro-osmosis. (b) Concentration profile at the resting potential. Bulk outflow from the inside of the membrane causes a low membrane conductance. (c) Concentration profile under a voltage-clamp depolarization. Inward volume flow gives a transient increase of the conductance. (d) Equivalent circuit of the membrane model.

tive fixed charges acts as a barrier between intracellular and extracellular compartments filled with electrolyte solutions. The external salt concentration c_1 is greater than the internal concentration c_2 , thus making it possible to associate the cation of the salt solution with sodium. The reason for choosing positive fixed charges in the channels is that this assumption leads to a conductance increase with membrane depolarization. A potential difference E applied across the membrane creates a convectional flow (i.e. bulk flow) with the linear velocity v (volume flow per unit of membrane area) by the process of electro-osmosis, in the presence of fixed charges, whose density is considered to be relatively low. A pressure difference P across the membrane may also be present to influence the volume flow.

Fig. 1b shows the concentration profile within a pore, when the axon is kept in the resting state by an externally created, resting potential difference E_r (negative at the inside). The pore is extended from 0 to δ in the x direction, perpendicular to the membrane surface. By electro-osmosis, a negative convection resting velocity v_r causes an upward concave concentration profile, resulting in a low conductance because of the low salt concentration in the pores. The concentration profile is determined by the combined processes of diffusion and convection. In Teorell's electrohydraulic analogue the outward volume flow v_r is thought to be compensated by a corresponding inward flow through uncharged "leaky pores", thus keeping the interior volume constant in the resting state (8, 10, 11, 12).

The effect of *depolarizing* the membrane by the application of a constant voltage step across the membrane (voltage clamp) is shown in Fig. 1c. If the inside of the membrane is made more positive (depolarization), the convection velocity will increase in the direction of the inside of the membrane. It is now assumed that the convection velocity will increase stepwise, due to the voltage step. The convection-velocity step will induce a relaxational change in the concentration profile. The membrane will be more filled with the highly concentrated salt solution from the external side of the membrane, causing a time-dependent increase of the conductance of the membrane.

Fig. 1d shows the *equivalent circuit* of the model. The concentration difference across the membrane and differences in ionic mobilities causes a diffusion potential E_d . Connection to the external potential difference E produces a current I through the mem-

brane. The following sign conventions have been adopted. The potentials (E and E_d) are measured internally, relative to the external value. The pressure difference P is the external pressure minus the internal. v is positive when directed inwards, while I is positive outwards. The conductance G of the membrane is defined from the integrated Nernst-Planck equations by the following relation:

$$I = G(E - E_d) \tag{1}$$

The conductance is dependent on the time and the voltage, as discussed above. The current I will be directed inward (negative) i.e. corresponding to the "early inward current", as long as E_d exceeds E . In order to conform with the Hodgkin-Huxley model, E_d should be positive and have a value corresponding to the sodium potential E_{Na} (see below).

Mathematical analysis of the convection-diffusion model

The mathematical treatment of a one-dimensional membrane model, taking into consideration both diffusion and convection, has been described in a previous publication (13) and will here be only briefly reviewed.

The concentration $c(x, t)$ inside a pore in the membrane, according to Fig. 1, is given by the following partial differential equation:

$$\frac{\partial c(x, t)}{\partial t} = D \frac{\partial^2 c(x, t)}{\partial x^2} - v(t) \frac{\partial c(x, t)}{\partial x} \tag{2}$$

where x is the space co-ordinate perpendicular to the membrane surfaces, t is time, $c(x, t)$ is the concentration as a function of x and t , D is the diffusion coefficient, and $v(t)$ is the linear convection velocity.

The application of a step voltage across the membrane from an initial value of E_1 volts to a new value of E_2 volts causes a step variation of the linear convection velocity from v_1 to v_2 , as discussed above. The corresponding transient change in the concentration profile is obtained from eq. (2). An analytical solution can be found and expressed in normalized quantities:

$$C(X, T)_{v_1 \rightarrow v_2} = C(X, \infty) + 2(1 - C_2) \frac{e^{V_1 X/2}}{1 - e^{V_1}} \times e^{-(V_2/2)^2 T} \sum_1^\infty \alpha_n e^{-(n\pi)^2 T} \sin n\pi X \tag{3}$$

where

$$C(X, \infty) = \frac{e^{V_1 X} - e^{V_2}}{1 - e^{V_1}} (1 - C_2) + C_2$$

and

$$\alpha_n = n\pi \left[\frac{1}{(V_1 - V_2/2)^2 + (n\pi)^2} - \frac{1}{(V_2/2)^2 + (n\pi)^2} \right] \times [1 - (-1)^n e^{(V_1 - V_2/2)}]$$

The following normalizations have been introduced:

$$X = x/\delta \quad (\delta = \text{membrane thickness}),$$

$$T = tD/\delta^2,$$

$$C_2 = c_2/c_1 \quad (c_1 = \text{extracellular concentration and } c_2 = \text{intracellular concentration}),$$

$$V_1 = v_1\delta/D,$$

$$V_2 = v_2\delta/D,$$

$$C(X, T) = c(X, T)/c_1 \text{ and}$$

$$C(X, \infty) = c(X, \infty)/c_1 = \text{steady-state concentration profile at infinite time (cf. ref. 16).}$$

The normalized conductance of the membrane is given by the following equation (17):

$$G(T) = 1 / \int_0^1 \frac{dX}{C(X, T)} \tag{4}$$

which is related to the total membrane conductance $g(T)$ by $G(T) = g(T)\delta/\lambda c_1$.

The constant λ is given by the following expression for the case of a monovalent single salt:

$$\lambda = F^2(u_+ + u_-) \tag{5}$$

where u_+ is the molar mobility of the cation ($\text{cm}^2 \text{ mol/joule sec}$), u_- is the molar mobility of the anion ($\text{cm}^2 \text{ mol/joule sec}$) and F is the Faraday constant.

The transient behaviour of the conductance of the membrane under a voltage clamp can thus be calculated from eq. (4), using eq. (3). The accompanying early current is given by eq. (1).

The influence of different values of the convection velocity V on the concentration and resistivity steady-state profiles inside the membrane is shown in Fig. 2. The curves were calculated from $C(X, \infty)$ in eq. (3) with $C_2 = 0.01$.

The Hodgkin-Huxley model

From experimental observations, using the voltage-clamp technique on the giant axon of Loligo, Hodg-

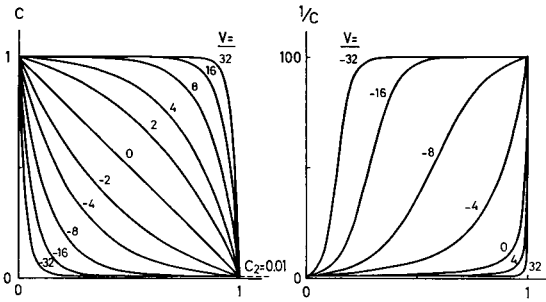


Fig. 2. (a) Steady-state concentration profiles of the convection-diffusion model at different normalized convection velocities V . $C_2=0.01$. (b) The inverse concentration from a proportional to the resistivity of the membrane. Integration of these curves in the x direction corresponds to the overall membrane resistance.

kin & Huxley (1) proposed that the membrane current was composed of a capacitive current and three ionic currents for potassium, sodium and other ions:

$$I = C_M \frac{dE}{dt} + \bar{g}_K n^4 (E - E_K) + \bar{g}_{Na} m^3 h (E - E_{Na}) + \bar{g}_l (E - E_l) \quad (6)$$

where I is the total membrane-current density (outward current positive), C_M is the membrane capacity per unit area, E is the membrane potential (depolarization positive), E_K , E_{Na} and E_l are the equilibrium potentials for potassium, sodium and other ions, \bar{g}_K , \bar{g}_{Na} and \bar{g}_l are the maximum conductances per unit area associated with the different ionic currents, and n , m , and h are continuous functions of membrane potential and time.

The sign convention used in eq. (6) is the opposite to that which Hodgkin & Huxley adopted but follows the most generally used sign convention for cell-membrane potentials.

Under a voltage clamp, the capacitive current is zero, since $dE/dt=0$, except for a very fast capacitive surge during the voltage step. Hodgkin & Huxley associated the parameters n , m and h with "potassium on" (potassium activation), "sodium on" (sodium activation) and "sodium off" (sodium inactivation) respectively. The terms "on" and "off" refer to increasing and decreasing membrane permeability (conductance). The permeability parameters n , m and h were assumed to satisfy first-order differential equations. The rate constants of these equations were determined by fitting the equations to experimental data. The process of sodium activation was thus described by the following equations:

$$\left. \begin{aligned} m &= m_\infty - (m_\infty - m_0) \exp(-t/\tau_m), \\ m_\infty, m_0 &= \alpha_m / (\alpha_m + \beta_m), \\ \tau_m &= 1 / (\alpha_m + \beta_m), \\ \alpha_m &= 0.1 (E_r - E + 25) / \left(\exp \frac{E_r - E + 25}{10} - 1 \right), \\ \beta_m &= 4 \exp \frac{E_r - E}{18}. \end{aligned} \right\} \quad (7)$$

Similar equations were applied as a description of the parameters n and h . The sodium activation is fast, compared with the other processes. Thus the kinetic behaviour of the early current I_0 will be determined by the following relation:

$$I_0 = \bar{g}_{Na} m^3 h_0 (E - E_{Na}) + \bar{g}_K n_0^4 (E - E_K) + \bar{g}_l (E - E_l) \quad (8)$$

where $\bar{g}_{Na} m^3 h_0$ represents the time-variant and non-linear conductance of the early current and h_0 and n_0 represent the initial values of h and n and are considered for the present purpose as time-invariant. Using $\bar{g}_{Na} = 120$ m mho/cm², $\bar{g}_K = 36$ m mho/cm² and $\bar{g}_l = 0.3$ m mho/cm², as given by Hodgkin & Huxley (1), the three ion conductances in eq. (8) at the steady-state resting potential $E_r = -65$ mV can be calculated as follows: $\bar{g}_{Na} m_0^3 h_0 = 0.0106$ m mho/cm², $\bar{g}_K n_0^4 = 0.367$ m mho/cm² and $\bar{g}_l = 0.3$ m mho/cm² (see Hodgkin & Huxley (1) for the equations describing n and h). It will be seen that the potassium and leakage conductances predominate over the sodium conductance at the resting potential. The maximum conductance of the early current when h and n are kept constant is about $\bar{g}_{Na} h_0 = 72$ m mho/cm². Thus the sodium conductance at the resting potential is a very small fraction of this maximum conductance, compared with the sum of the potassium and leakage conductances at the resting potential, which is about 1% of the maximum conductance. These figures will be used in discussing the calculations below.

COMPUTATIONS AND RESULTS

In the following pages the abbreviations "CD" and "HH" will be used for "convection-diffusion" and "Hodgkin-Huxley" respectively.

The transient conductance of the CD model has been calculated from eqs. (3) and (4) for a number of values of the initial and final convection velocity, V_1 and V_2 , corresponding to a step in the clamping

Table. I. Summary of the different cases shown in Figs. 3-6.

Fig. 3.	Linear scale	Fig. a.	Hodgkin-Huxley	$E_r = -65$ mV	
Fig. 4.	Log scale	Fig. b.	Convection-diffusion	$\left\{ \begin{array}{l} V_r = -10 \\ V_r = -16 \\ V_r = -6 \\ V_r = -10 \end{array} \right\}$	$C_2 = 0.01$
Fig. 5.	Linear scale	Fig. c.			
Fig. 6.	Log scale	Fig. d.			
		Fig. e.			

voltage. Also the ratio C_2 of the intracellular and the extracellular salt concentrations has been varied.

The results have been compared with the kinetic behaviour of the conductance of the early current in the HH theory. Calculations have been made of the conductance associated with the activation process of the sodium permeability caused by a change of the membrane potential from E_1 to E_2 . The conductance was calculated as $\bar{g}_{Na} m^3 h_0$ (cf. eq. (8)), using eq. (7). The following numerical values from HH were used: $\bar{g}_{Na} = 120$ m mho/cm², $E_r = -65$ mV, $h_0 = 0.596$, ($E_{Na} = 50$ mV).

The numerical calculations were made on a Control Data 3600 digital computer. Details of the numerical methods used in the calculations on the CD model have been given in a previous publication (13).

Early conductance changes during voltage clamp

1. *General.* Figs. 3-6 show the conductance, corresponding to the early current, as a function of time, when a voltage step is applied across the model membrane. As mentioned above, the voltage step corresponds to a convective step in the CD model. The various conditions under which these figures have been calculated are summarized in Table I. Figs. 3 and 4 have been calculated for the case of depolarization of the membrane from the resting potential. In Fig. 3 the conductance has been plotted on a linear scale, and in Fig. 4 the difference between the time-variant conductance and the steady-state conductance at infinite time is shown on a logarithmic scale. Figs. 5 and 6 show repolarization back to the resting potential on the linear conductance scale and the log scale respectively. In Figs. 3-6 the results from the HH model are given in *a* and from the CD-model in *b-e*. *b-d* have been calculated for $C_2 = 0.01$ and show the influence of different values of the convection velocity V_1 corresponding to the resting potential. In *b*, *c* and *d*, $V_1 = -10$, -16 and -6 respectively. *b* and *e*, finally,

show the effect of varying C_2 , which is 0.01 in *b* and 0.1 in *e*, while keeping the resting velocity V_1 at a constant value, $V_1 = -10$.

2. *Depolarization.* Fig. 3 shows that the transient increase of the conductance, from a low conductance state at the resting potential to a high conductance when the membrane is depolarized, is sigmoidal in shape for both the HH and the CD model. Another common feature of the two models is that the time constant is low for small and large depolarizations but high for medium depolarizations. These properties are also seen on the log scale in Fig. 4. The convex appearance of the curves in Fig. 4 corresponds to the sigmoidal shape in Fig. 3. That the time constant has a maximum for medium depolarizations will be inferred from Fig. 4, by comparing the slopes of the curves under different degrees of depolarization.

The effect of varying the initial convection velocity V_1 will be seen in Figs. 3-4, *b-d*. Decreasing the initial velocity decreases the value of the initial conductance and makes the sigmoidal shape of the conductance transient more pronounced. The situation will be the opposite when the initial velocity has an increased value. This is also a property of the HH model, when the initial potential E_1 is varied.

The effect of the concentration ratio C_2 can be studied in Figs. 3-4, *b* and *e*. A high value of C_2 gives a high initial conductance and a less pronounced sigmoidal shape. The former property is due to the fact that the low conductance state is created by the inflow of the low-concentration salt solution from the interior of the membrane. A high value of the inner concentration thus corresponds to a high conductance in the resting state.

3. *Repolarization.* When the membrane is repolarized, the conductance change is approximately exponential in both the HH and the CD models, as shown in Figs. 5 and 6. Hodgkin & Huxley were uncertain about the extent to which the rate of return of the sodium conductance could be regarded as

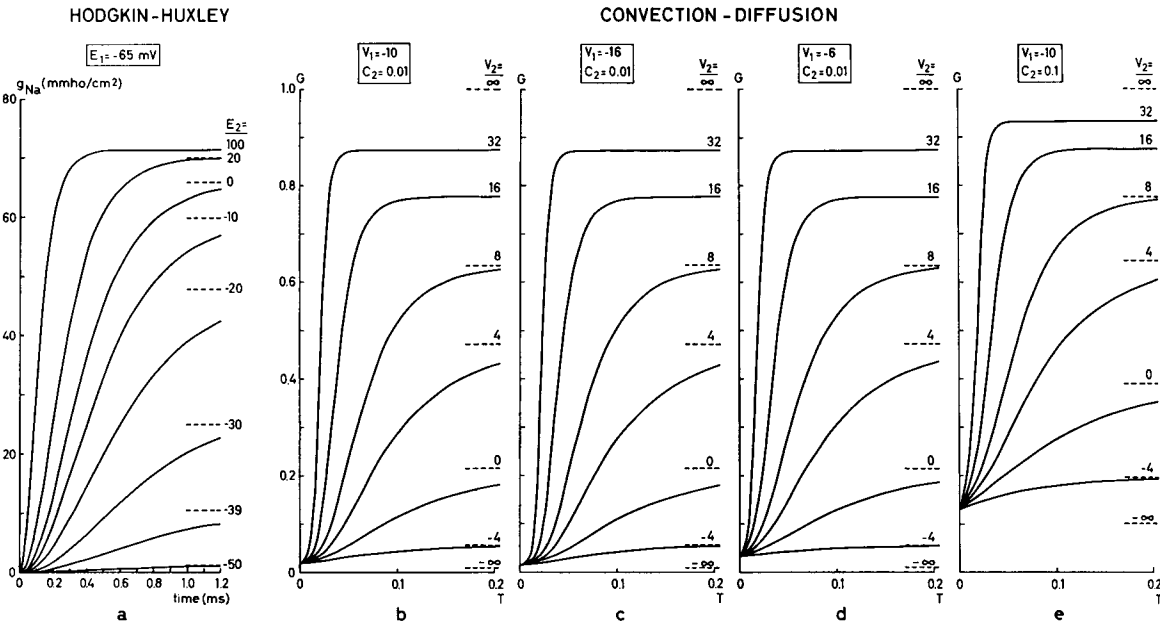


Fig. 3. Transient conductance changes associated with the early current under depolarization. *a* was calculated from the Hodgkin-Huxley theory of sodium activation and *b-e* from the convection-diffusion model. Note the sigmoidal shape in both models and the voltage (or convection-velocity) dependence of the time constant.

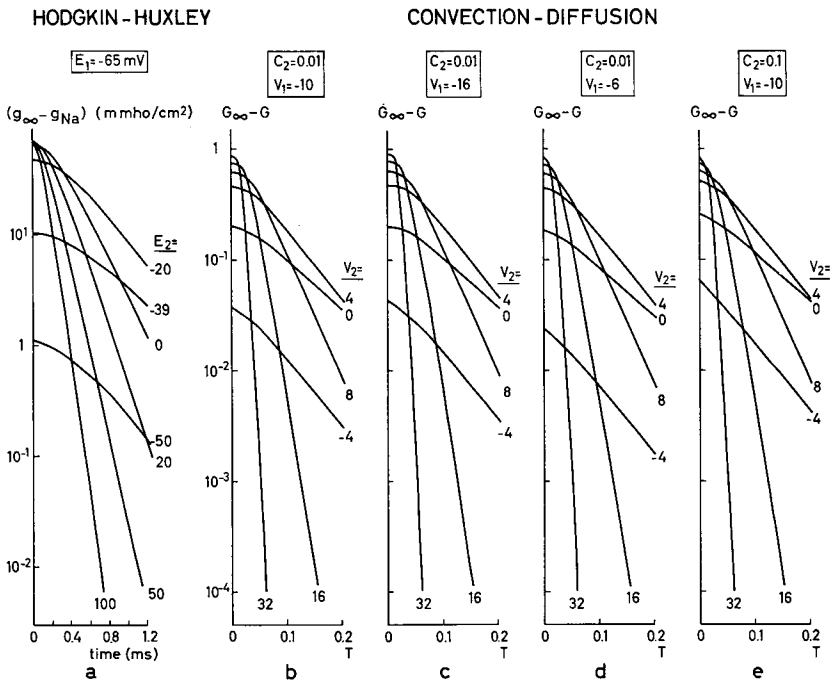


Fig. 4. Same as Fig. 3 but with the final steady-state conductance G_{∞} minus the time-dependent conductance G on a logarithmic scale on the ordinate.

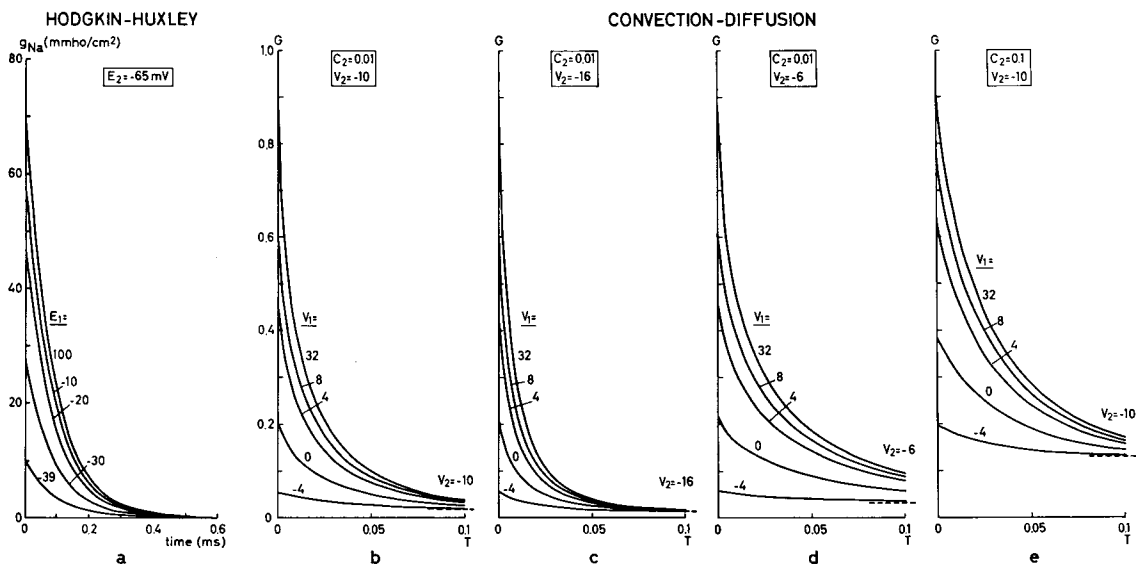


Fig. 5. Transient conductance changes associated with the early current under repolarization back to the resting potential. *a* was calculated from the Hodgkin-Huxley theory of sodium activation and *b-e* from the convection-diffusion model. Note the approximately exponential time course.

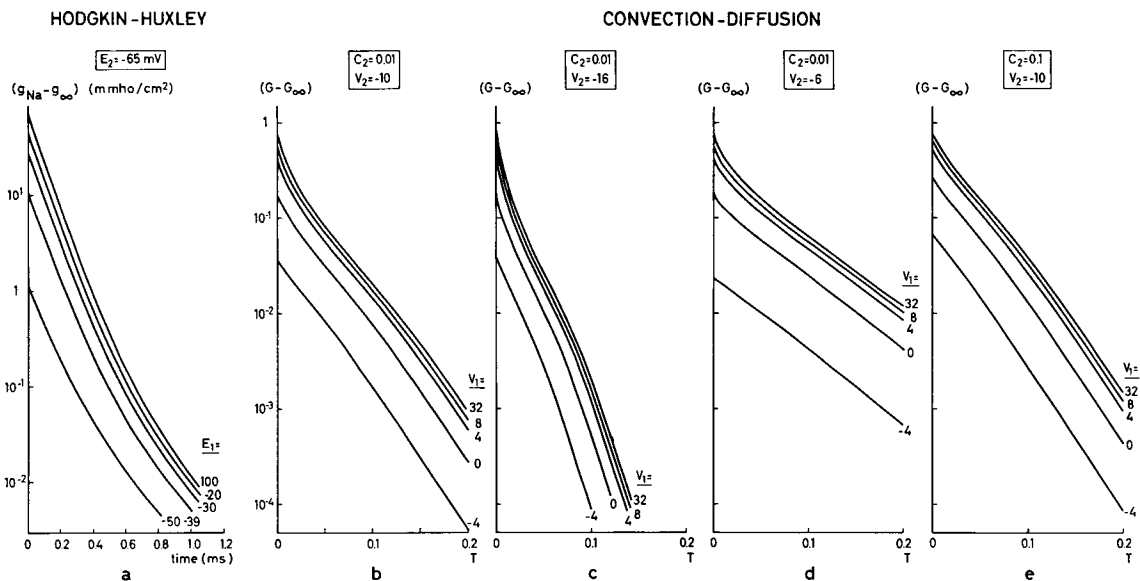


Fig. 6. Same as Fig. 5 but for the time-dependent conductance G minus the final steady-state conductance G_{∞} on the ordinate on a logarithmic scale. Note the approximately exponential time course and the fact that the time constant is approximately independent of the initial value of the membrane potential E_1 (or the convection velocity V_1) but dependent on the final values, E_2 and V_2 .

exponential in their experiments (p. 484 in ref. 18), since experimental errors probably influenced the measurements. However, one axon, which was in excellent condition, showed clear departures from

exponential behaviour in that the initial fall of conductance was too rapid. An interesting point is that this latter appearance is also a property of the CD model.

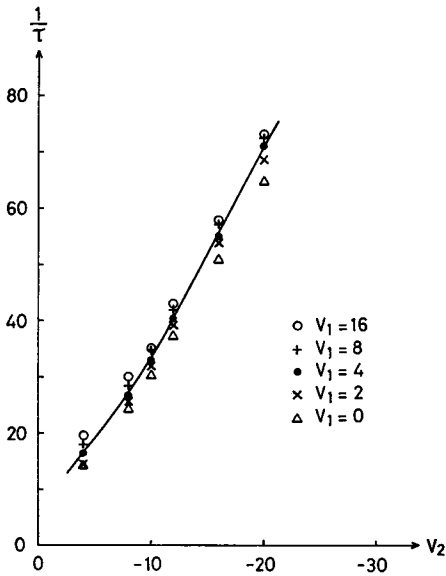


Fig. 7. The rate constant of the convection-diffusion conductance decay under repolarization as a function of the final convection velocity for different values of the initial velocity for a case with $C_2=0.1$. Note that the rate constant is approximately independent of the initial velocity.

The time constant of the conductance decay during repolarization is approximately independent of the initial potential in both models, as can be seen from the slopes of the curves in Fig. 6. The time constant of the decay is, however, greatly dependent on the final potential in both models. Low values of the final convection velocity produce a steeper decay (Figs. 5–6, *b–d*). The higher value of C_2 reduces the initial slope (Fig. 5, *b* and *e*) and gives a conductance decay which is closer to the exponential form (Fig. 6, *b* and *e*).

An example of the effect of varying the initial and final convection velocities on the rate constant $1/\tau$ of the decline of the CD conductance under repolarization is shown in Fig. 7. The time constant τ was calculated as the normalized time at which the conductance had decayed to $1/e$ of the initial value. The calculations were made for $C_2=0.1$. It will be clearly seen that the initial velocity V_1 has little influence on the rate constant, compared with the final velocity V_2 . Fig. 7 should be compared with a figure given by Hodgkin & Huxley (Fig. 9, p. 484, ref. 18) for the analogous experimental results on the giant axon. Both figures show considerable qualitative similarities.

4. *Resting conductance.* A main difference between the conductance curves calculated from the HH model and the CD model concerns the conductance at the resting potential. In the HH model the conductance $\bar{g}_{\text{Na}} m^3 h_0$ assumes a very small value at the resting potential, compared with the CD conductance (Figs. 3 and 5). However, this may be interpreted by assuming that the resting conductance in the CD model includes the conductances corresponding to the potassium and the leakage channels in the HH formulation. As discussed above, the potassium and leakage conductances constitute about 1% of the maximum conductance and may correspond to the CD conductance G at $V=-\infty$, which is equal to C_2 (see eq. (10) below). When $C_2=0.01$, this correspondence is satisfactory, though the remaining conductance in the CD model after the subtraction of C_2 is still high, as compared with the extremely low sodium conductance at the resting potential in the HH model.

Fitting the convection-diffusion model to the Hodgkin-Huxley equations

The conductance of the early current in the CD model can be fitted to the HH equations by formally comparing the conductance with the expression $\bar{g}_{\text{Na}} m^3 h_0$ (cf. eq. (8)), where m satisfies the first equation in eq. (7). From this comparison the equivalent time constant associated with different values of V_1 and V_2 can be calculated. With regard to the discussion above concerning the conductance at the resting potential, a time-independent conductance G_z is now introduced into the CD model. G_z corresponds to the sum of potassium and the leakage conductance at the resting potential in the HH theory and is subtracted from the CD conductance before the fitting procedure. The equation which was fitted to the CD conductance was thus given the following form (cf. eqs. (7) and (8)):

$$G_a = \left[\sqrt[3]{G_\infty - G_z} - (\sqrt[3]{G_\infty - G_z} - \sqrt[3]{G_0 - G_z}) \right]^3 \times \exp(-T/\tau) + G_z \quad (9)$$

where G_a is the approximate conductance, G_0 is the conductance at zero time for the CD model, G_∞ is the conductance at infinite time for the CD model, and τ is the approximate normalized time constant.

In accordance with the discussion above, the value of G_z was chosen as the steady-state con-

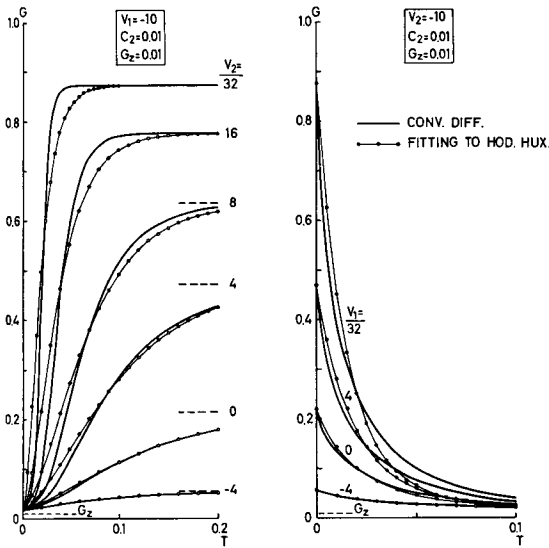


Fig. 8. An example of the application of curve-fitting to the convection-diffusion conductance. *a* is for depolarization and *b* for repolarization. Thick curve = conductance *G* of the convection-diffusion model. Thin curve = approximate conductance *G_a* in accordance with the Hodgkin-Huxley formalism (eqs. (9) and (10)).

ductance at infinite negative velocity in the CD model, $G_{V=-\infty}$. Thus from Fig. 1 and eq. (4), we have

$$G_z = G_{V=-\infty} = C_2 \tag{10}$$

The procedure of the fitting was as follows. The conductance *G* of the CD model was calculated at 10 or 20 discrete values of the time *T*, equally spaced between $T=0$ and $T=0.1$ or 0.2 . The value $T=0.1$ was used when the conductance transient was fast, and $T=0.2$ was chosen when the transient was slow. The values of G_0 and G_∞ were taken as the initial and final conductances of the CD model. The discrete values of the CD conductance were then fitted to eqs. (9) and (10) by the least-squares method. The sum of $(G - G_a)^2$ at the discrete points was minimized with respect to τ by means of digital computation.

The results of such a fitting are shown in Fig. 8 for $V_1 = -10$ and $C_2 = 0.01$ (cf. Figs. 3*b* and 5*b*). Fig. 8*a* shows the conductance transient due to depolarization, and Fig. 8*b* shows the conductance during repolarization. The thick curves are from the CD model and the thin curves are the approximation from eqs. (9) and (10). It will be seen in Fig. 8*a* that the approximations of the depolarization curves are less sigmoid than the original curves from the CD model. The approximate curves are also less sigmoid than the corresponding results

from the HH equations (Fig. 3*a*). This discrepancy is due to the fact that $(G_0 - G_z)$ is greater than the conductance of the giant axon at the resting potential. However, the fitting procedure makes it possible to compare the non-linear behaviour of τ_m as a function of E_1 and E_2 and the variation of τ with respect to V_1 and V_2 .

A comprehensive diagram of the main results of the CD model is given in Fig. 9. This figure shows the resulting time constants and steady-state conductances obtained by the above fitting procedure (Fig. 9*b-e*) and also the corresponding HH relations (Fig. 9*a*) for comparison. The parameter values chosen for the CD model in Fig. 9*b-e* are identical with those shown in Table I for *b-e*. In Fig. 9*a*, τ_m and m_∞ , calculated from eq. (7), have been plotted, and Figs. 9*b-e* show τ and M_∞ . M_∞ is defined by

$$M_\infty = \sqrt[3]{G_\infty - G_z} \tag{11}$$

M_∞ can be looked upon as corresponding to m_∞ , when eq. (9) is compared with the equation for *m* in eq. (7).

The continuous curves for the time constants in Fig. 9 have been calculated for the case of depolarization from the resting potential E_r to E in Fig. 9*a* and from the resting velocity V_r to V in Fig. 9*b-e*. The dashed curves correspond to the time constants, obtained for repolarization back to E_r and V_r from E and V respectively.

The salient features of Fig. 9 are as follows:

(1) In all the cases in Fig. 9*b-e*, the CD model qualitatively reproduces the time constants τ_m at depolarization in the HH model (Fig. 9*a*). It is interesting to note that in the HH model the depolarization time constant is only dependent on the final potential E and not on the initial potential E_r . Fig. 9*b-e* shows that this is also approximately true of the CD model.

(2) At repolarization the HH equations give a time constant τ_m (dashed curve in Fig. 9*a*) which is only dependent on the final potential E_r and independent of the initial potential E . This is also approximately a property of the CD model (Fig. 9*b-e*).

(3) A comparison of the steady-state conductance parameters M_∞ (Fig. 9*b-e*) and m_∞ (Fig. 9*a*) shows a general resemblance. The two main differences are the inability of M_∞ to reproduce the very low conductance state of m_∞ (in spite of the subtraction

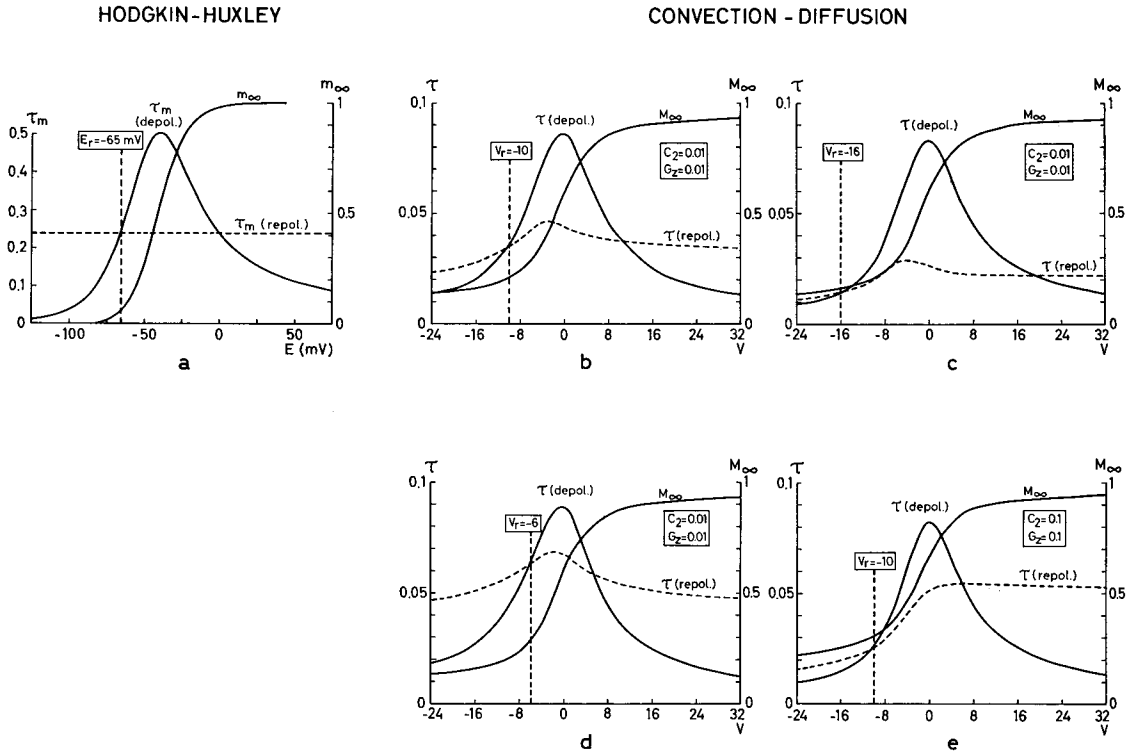


Fig. 9. Results of formal curve-fitting of the Hodgkin-Huxley theory to the convection-diffusion model (b-e). For comparison, the sodium activation parameters of the

Hodgkin-Huxley equations are shown in a, when the resting potential $E_r = -65$ mV. τ and M_∞ in b-e are given by eqs. (9) and (11).

of G_2) and the fact that M_∞ approaches its maximum value much more slowly than m_∞ . These discrepancies between the models were also apparent in Fig. 3.

If the different figures in Fig. 9 are compared, the best approximation to the HH model with the resting potential $E_r = -65$ mV (Fig. 9a) is considered to be Fig. 9b, with $V_r = -10$ as the convection velocity at the resting potential and with $C_2 = 0.01$.

The details of this matching are given in the Appendix and the results are summarized in Table II. The accuracy of the estimations in Table II is probably fairly high, as regards the diffusion coefficient D and the molar mobility u . The other parameters are considered to be within about an order of magnitude. The results in Table II will be commented on in the Discussion section.

QUANTITATIVE ESTIMATION OF SOME MODEL PARAMETERS

A quantitative comparison of the HH model and the CD model has been made out in order to estimate the values of some parameters of the CD-model necessary for compatibility with the squid-axon data. Fig. 9a and b has been used for this purpose. The quantitative correspondence between these two figures was established by matching the following scales:

- (1) τ and τ_m scales,
- (2) M_∞ and m_∞ scales,
- (3) V and E scales.

DISCUSSION

THE EARLY INWARD CURRENT

Qualitative aspects

The qualitative comparison between the CD model of the early current under the voltage clamp and the HH-model of the sodium activation can be summarized as follows:

Similarities. 1. Sigmoidal conductance change from a low value to a high value as a function of time when the membrane is depolarized.

Table II. Quantitative estimation of parameters of the CD-model

Parameter	Symbol	Approximate value
Diffusion coefficient	D	$1.7 \cdot 10^{-10} \text{ cm}^2/\text{sec}$
Molar mobility	u	$0.74 \cdot 10^{-13} \text{ cm}^2 \text{ mol}/\text{joule sec}$
$D/D_{\text{free}} = u/u_{\text{free}}$		$1.1 \cdot 10^{-5}$
Pore area/membrane area	α	0.1
Internal concentration	c_1	520 mM
External concentration	c_2	5.2 mM
Outward volume flow from electro-osmotic channels at resting potential	J_v	170 nl/sec cm^2
(Electrical conductance) \times (electro-osmotic permeability)	$\kappa' \beta = l$	0.0047 cm/sec V
Electro-osmotic permeability	β	0.64 mV/cm H_2O
Mechanical conductance	$Lp + \kappa' \beta^2 = s$	$3.0 \cdot 10^{-6} \text{ cm}/\text{sec cm H}_2\text{O}$
External pressure at resting potential	P	44 cm H_2O
Fixed-charge density	\bar{X}	1.6 mM

2. Maximum time constant of the conductance change for medium depolarizations and decreasing time constant for lower and higher values of the depolarization voltage. The time constant is independent of the initial membrane potential and is determined only by the final value of the potential.

3. Approximate exponential time course of the conductance when the membrane is repolarized.

4. Time constant of the conductance change on repolarization approximately independent of the initial voltage but dependent only on the final voltage.

5. Sigmoidal steady-state conductance as a function of membrane potential.

Discrepancies. 1. The steady-state conductance at and below the resting potential is smaller in the HH model, as compared with the CD model.

2. The steady-state conductance approaches its maximal value at high values of the potential more slowly in the CD model than in the HH model.

The *similarities* include all the important *kinetic properties* of the sodium activation. These characteristics are highly non-linear and do not seem to have been demonstrated on earlier models.

The *discrepancies* concern mainly the *steady-state properties* and may possibly be connected with approximations of the CD model. For example, interactions with the walls of the pores have not been included in the model, nor the three-dimensional aspects of the membrane transport. As discussed

in the introduction, the equations used in the CD model are appropriate for a macroscopic case but may not be valid on the microscale for a cell membrane. If the physical basis of the equations is doubtful, it may be valuable to look upon the mathematical formulation as "operational". It may also be possible to find other physical interpretations of the CD equations, such as the analogy with the constant-field single-ion electrodiffusion regime (3, 13). However, the latter analogy is not compatible with a sodium channel, as regards the early current (3).

The CD model assumes some sort of *selectivity*, since the internal and external salt concentrations should be different. The model is compatible with sodium permeation, but the anion will be more difficult to identify, if E_a in eq. (1) is to correspond to E_{Na} in the HH theory. The evidence for the existence of selective ionic channels in nerve membranes have been reviewed by Hille (19), but the presence of separate ion channels has also been questioned (20).

Quantitative aspects

The low value of the *mobility* u in Table II with respect to that of a free solution corresponds to the low mobility for potassium in electrodiffusion models, as given by Cole (3). As regards the CD model, however, the low mobility may correspond to interaction with the walls of the pores and thus may interfere with the assumption of bulk flow and

electro-osmosis. The size and population of the equivalent pores of the axolemma of the squid have been measured by Villegas, Bruzual & Villegas (21). They found that the equivalent pores have a radius of 5–6 Å and are spaced about 1 000 Å apart. This corresponds to a *relative pore area* $\alpha \approx 10^{-4}$, which may be compared with $\alpha = 10^{-1}$ given in Table II. $\alpha = 10^{-4}$ is unattractive in the CD model, since it would mean a very high value of c_1 , which is inversely related to α (cf. eq. (A6)).

The discrepancy between the α values of the CD model and those obtained from measurements may be explained by the model suggested by Teorell (10) with the excitable unit within the membrane itself. This may also explain the rather high membrane *pressure difference* of the CD model (Table II). Theoretically this has been predicted by Schlögl (22). Teorell (23) found experimentally pressure gradients within model membranes under zero transmembrane pressure. A model with these properties has also recently been discussed by Forster (15). It may also be mentioned that Agin (24) suggests the possibility of a high hydrostatic pressure within an electrodiffusion membrane, though the transmembrane pressure difference is zero. As regards the *concentrations*, c_1 and c_2 may be quite different from the extracellular and intracellular concentrations. Concentration gradients may be built up in the membrane even with a zero total concentration difference, as shown by Teorell (9).

The β value (*electro-osmotic permeability*) in Table II is within an order of magnitude, compared with measurements made by Vargas (25), who found $\beta = 0.041$ mV/cm H₂O in the squid. The positive *fixed-charge density* \bar{X} of the CD model (Table II) may be compared with measurements made by Vargas (25), who obtained -10 meq/litre as a value of the fixed-charge density of the squid-axon membrane. However, the membrane might be heterogeneous and the measurements are in that case only reflecting the net sum of positive and negative sites, as Vargas pointed out.

THE LATE OUTWARD CURRENT

The present model does not include the mechanism of the late outward current corresponding to the sodium inactivation and potassium activation in the HH theory.

In Teorell's excitability analogue the late outward current (though in fact directed inward in Teorell's model) corresponds to what may be regarded as a

pressure relaxation. During this process there is a slow variation in the pressure, under the influence of geometrical factors, causing a continuous change of the convection velocity V . The concentration profiles, although changing with time, approach the steady-state requirements of the conductance with respect to the CD process (cf. Fig. 8 in ref. 8). The non-linearities, which are essential for a comparison with the HH equations, enter mainly in the following two equations, given by Teorell (12):

$$(1) M = f(P),$$

$$(2) R^\infty = f(V).$$

The first equation describes the internal volume M as a function of the transmembrane pressure difference P and the second equation is the "backbone curve", giving the steady-state resistance R^∞ as a function of the convection velocity V . The "backbone curve" is calculated from $C(X, \infty)$ in eq. (3) and eq. (4) (7). However, the first relation $M = f(P)$ is unknown (12), and calculations of the late outward current can only be made in special cases. One special case is $M \propto P$, which under a voltage clamp gives a simple solution as a first-order differential equation in V (eq. (6) in ref. 8) with an exponential solution. This solution, in combination with the backbone curve, will probably show interesting non-linear behaviour, but the translation to the HH equations is somewhat complicated by the fact that the pressure relaxation corresponds to both the h ("sodium off") and n ("potassium on") parameters.

As concerns electrodiffusion models, Cole (3) has discussed the possibility of explaining potassium behaviour by a *single-ion electrodiffusion theory*. It may also be adequate to consider a single-ion electrodiffusion model for the sodium inactivation. These possibilities of reproducing the behaviour of the late outward current in single-ion electrodiffusion models will be dealt with in a subsequent paper.

ACKNOWLEDGEMENTS

I wish to thank Professor T. Teorell for his encouragement and help during this investigation. I am also greatly indebted to Dr J. Sandblom for numerous substantial suggestions and enlightening discussions throughout the work. The careful drawing of the figures by H. Billander is appreciated. I also want to thank Mrs E. Arnelund for skilful editorial work.

This work was supported by the Medical Faculty of the University of Uppsala, the Swedish Medical Research Council (Project No. 14X-629) and the National Institutes of Health (Grant No. 5, R01, HE12960-08).

APPENDIX

ESTIMATION OF MODEL PARAMETERS

In this Appendix the quantitative comparison between the HH model (Fig. 9a) and the CD model (Fig. 9b) will be described.

1. Time constants τ and τ_m

The relation between the time constants τ (CD) and τ_m (HH) is given by the following normalization expression (see under eq. (3)):

$$\tau = \tau_m D / \delta^2 \tag{A1}$$

The scales of the time constants in Fig. 9a and b can be matched by equalizing the maximum values, which are $\tau_m = 0.5$ msec and $\tau = 0.086$ respectively. Here and in the following text $\delta = 100 \text{ \AA}$ will be used. These values used in eq. (A1) give an estimation of the total diffusion constant D of the salt solution in the membrane and the corresponding molar mobility $u = D/RT$ (R =gas constant and T =absolute temperature = 279°K):

$$D = 1.7 \cdot 10^{-10} \text{ cm}^2/\text{sec} \tag{A2}$$

$$u = 0.74 \cdot 10^{-13} \text{ cm}^2 \text{ mol}/\text{joule sec} \tag{A3}$$

If the salt solution is considered to be NaCl, the values of the diffusion coefficient and the mobility can be compared with those in a free solution:

$$D/D_{\text{free}} = u/u_{\text{free}} = 1.1 \cdot 10^{-5} \tag{A4}$$

The diffusion coefficient in a free solution of NaCl was taken as $D_{\text{free}} = 1.5 \cdot 10^{-5} \text{ cm}^2/\text{sec}$.

2. Steady-state conductance parameters M_∞ and m_∞

The m_∞ curve (Fig. 9a) and the M_∞ curve (Fig. 9b) correspond to the steady-state conductances of the two models. The quantitative comparison is established by matching the maximum conductances (cf. eqs. (4), (5) and (8)):

$$\bar{g}_{\text{Na}} m_\infty^3 h_0 = G_\infty F^2 (u_+ + u_-) c_1 \alpha / \delta \tag{A5}$$

in which α (=pore area/membrane area) was introduced, since the CD conductance refers to the pores only, but the sodium conductance in the HH formulation is given relative to the whole axon membrane. With numerical values ($m_\infty = 1$, $\bar{g}_{\text{Na}} h_0 = 0.0715 \text{ mho}/\text{cm}^2$, $G_\infty = 1$ and $u_+ \approx u_- \approx u$ according to eq. (A3)) eq. (A5) gives

$$c_1 = 52/\alpha \text{ mM} \tag{A6}$$

If the cation in the salt solution is considered to be sodium, then c_1 may correspond to the blood concentration of sodium in the squid, which is 440 mM (26). Thus from eq. (A6)

$$\alpha \approx 0.1 \tag{A7}$$

This α value will be used in the calculations below.

The outward volume flow J_v associated with the CD pores (expressed per cm^2 axon-membrane area) at the resting potential ($V = -10$) can now be calculated as

$$J_v = \alpha V D / \delta = -0.17 \text{ } \mu\text{l}/\text{sec cm}^2 \tag{A8}$$

3. Convection velocity V and potential E

The relation between V and E is given by the following thermodynamic expression (7, 27):

$$J_v = \kappa' \beta E + (L_p + \kappa' \beta^2) P \tag{A9}$$

where

$\kappa' = (I/E)_{P = \pi = \pi_s = 0}$ = electric conductance

$\beta = -(E/(P - \pi))_{\pi_s = I = 0}$ = electro-osmotic permeability (streaming potential)

$L_p = (J_v/(P - \pi))_{\pi_s = I = 0}$ = filtration coefficient.

The following symbols were used: π = total osmotic-pressure difference, π_s = osmotic-pressure difference of permeable solute. Teorell (7, 27) uses the abbreviations $l = \kappa' \beta$ and $s = L_p + \kappa' \beta^2$ in eq. (A9).

The V and E scales in Fig. 9a and b are matched by comparing the widths ΔV and ΔE of the τ and τ_m curves at half of the maximum values. It is found that $\Delta V = 16.8$ and $\Delta E = 62$ mV. During CD relaxation, the transmembrane pressure P is considered to be constant. Thus from eq. (A9)

$$\kappa' \beta = \Delta J_v / \Delta E = \alpha \Delta V D / \delta \Delta E = 0.0047 \text{ cm}/\text{sec V} \tag{A10}$$

The orientation of the τ and τ_m curves (Fig. 9a and b) along the E and V axes is determined by the choice of the pressure difference P . If the resting potential $E = -65$ mV corresponds to $V = -10$, eqs. (A8), (A9) and (A10) give:

$$P(L_p + \kappa' \beta^2) = 1.3 \cdot 10^{-4} \text{ cm}/\text{sec} \tag{A11}$$

The fixed-charge density \bar{X} is given by the following expression (22):

$$\bar{X} = \kappa' \beta / (L_p + \kappa' \beta^2) F \quad (\text{A12})$$

In order to calculate P and \bar{X} , the values of κ' and L_p must be known. κ' can be calculated from the CD model, according to the definition under eq. (A9). At the resting potential, $P=0$ would correspond to a large outward volume flow with $G \approx G_2$, corresponding to $\kappa' \approx 0.715 \cdot 10^{-3}$ mho/cm². From eq. (A10) this value gives $\beta = 0.64$ mV/cm H₂O and $\kappa' \beta^2 = 3.0 \cdot 10^{-6}$ cm/sec cm H₂O. L_p will be taken from measurements by Vargas (28), who obtained $L_p = 3.2 \cdot 10^{-8}$ cm/sec cm H₂O for the intact squid axon. It may be noticed, however, that this L_p value is an average value for the whole axon membrane and may not be adequate to characterize the osmotic channels according to the CD model. However, using these numerical values in eqs. (A11) and (A12) results in $P = 44$ cm H₂O and $\bar{X} = 1.6$ mM. The results of the calculations above are shown in Table II.

REFERENCES

1. Hodgkin, A. L. & Huxley, A. F.: *J Physiol* 117: 500, 1952.
2. Cole, K. S.: *Membranes, Ions and Impulses*. Berkeley and Los Angeles, University of California Press, 1968.
3. Cole, K. S.: *Physiol Rev* 45: 340, 1965.
4. Mackey, M. C. & McNeel, M. L.: *Biophys J* 11: 664, 1971.
5. Sandblom, J.: *Biophys J*, in press.
6. Teorell, T.: *J Gen Physiol* 42: 831, 1959.
7. Teorell, T.: *J Gen Physiol* 42: 847, 1959.
8. Teorell, T.: *Acta Soc Med Upsalien* 65: 231, 1960.
9. Teorell, T.: *Arkiv för Kemi* (published by the Roy Swed Acad Sci) 18: 401, 1961.
10. Teorell, T.: *Biophys J* 2: 27 s, 1962 (suppl.).
11. Teorell, T.: *Ann N Y Acad Sci* 137: 950, 1966.
12. Teorell, T.: *In Handbook of Sensory Physiology* (ed. W. R. Loewenstein), vol. I, p. 291. Springer-Verlag, Berlin, Heidelberg and New York, 1971.
13. Hägglund, J. V.: *Uppsala J Med Sci*, in press.
14. Solomon, A. K.: *J Gen Physiol* 51: 335 s, 1968 (suppl.).
15. Forster, R. E.: *In Current Topics in Membranes and Transport* (ed. F. Bronner and A. Kleinzeller), vol. 2, p. 41. Academic Press, 1971.
16. Manegold, E. & Solf, K.: *Kolloid-Z* 59: 179, 1932.
17. Labes, R.: *Z Biol* 93: 42, 1932.
18. Hodgkin, A. L. & Huxley, A. F.: *J Physiol* 116: 473, 1952.
19. Hille, B.: *In Progress in Biophysics and Molecular Biology*. Ed. J. A. V. Butler and D. Noble, vol. 21, p. 1, 1970.
20. Tasaki, A.: *Nerve Excitation: a Macromolecular Approach*. C. C. Thomas, Springfield, 1968.
21. Villegas, R., Bruzual, I. B. & Villegas, G. M.: *J Gen Physiol* 51: 81 s 1968 (Suppl.).
22. Schlögl, R.: *Z Physikal Chem* 3: 73, 1955.
23. Teorell, T.: personal communication.
24. Agin, D.: *Proc N A S* 57: 1232, 1967.
25. Vargas, F. F.: *J Gen Physiol* 51: 123 s, 1968 (suppl.).
26. Hodgkin, A. L.: *The Conduction of the Nervous Impulse*, Liverpool University Press, 1971.
27. Caplan, S. R. & Mikulecky, D. C.: *In Ion Exchange* (ed. J. A. Marinsky), vol. 1, p. 1. Marcel Dekker, Inc., New York, 1966.
28. Vargas, F. F.: *J Gen Physiol* 51: 13, 1968.

Received February 24, 1972

Address for reprints:

Jarl Hägglund BM
Institute of Physiology and Medical Biophysics
Biomedical Centre, Box 572
S-751 23 Uppsala
Sweden